Spectroscopic and Theoretical Determination of the Electronic Structure of Thiazyl Chains and Extrapolation to Poly(sulfur nitride), $(SN)_x$: A Contribution to the Study of Conducting Polymers

Alberto Modelli,* Marco Venuti, Francesco Scagnolari, and Michele Contento

Dipartimento di Chimica "G. Ciamician", Università di Bologna, via Selmi 2, 40126 Bologna, Italy

Derek Jones

ICoCEA, Consiglio Nazionale delle Ricerche, via Gobetti 101, 40129 Bologna, Italy

Received: July 19, 2000; In Final Form: October 11, 2000

The filled and empty level structures of the thiazyl chains R−NSN−R and $(R-NSN)_2S$, with R = $Si(CH_3)_3$, are investigated by means of ultraviolet photoelectron and electron transmission spectroscopy. The spectral features are interpreted with the support of ab initio Hartree−Fock (HF)/6-31G* and semiempirical AM1 calculations, within the Koopmans' theorem approximation, and with density functional theory, using the orbital energies of the transition state electronic configuration. Post-HF calculations with infinite-order coupled-cluster expansion are employed to evaluate the first vertical electron affinity value of R−NSN−R, with R = H and CH_3. The experimental and theoretical results obtained for the thiazyl chains, as well as those for *trans*-oligoethenes, are extrapolated in order to evaluate the first ionization energy and electron affinity values for the corresponding (ideal) gas-phase polymers. Poly(sulfur nitride) is predicted to possess a smaller ionization energy and a sizeably higher electron affinity than those of *trans*-polyacetylene, with a consequent greatly reduced highest occupied molecular orbital−lowest unoccupied molecular orbital energy gap, in agreement with its highly conductive nature.

Introduction

Poly(sulfur nitride), $(SN)_x$, is a one-dimensional polymer which displays exceptional conducting properties along the π chain, where the alternating sulfur and nitrogen atoms donate two electrons and one electron, respectively.[1,2] This material, which also behaves as a superconductor below liquid-helium temperature, was the first example of a polymeric metal. Its conductivity (10^3 S cm^{-1}) at room temperature is 5 orders of magnitude larger than that of *trans*-polyacetylene.[3] In addition, $(SN)_x$ possesses a high electronegativity, because of which the polymer can be employed to increase the efficiency of GaAs solar cells[4] or as a catalyst.[5]

Long-range intramolecular electron-transfer processes are increasingly important in chemistry, biochemistry, and in particular the field of nanoscale technology and molecular devices.[6] In particular, a delocalized π system capable of transmitting variations of charge density between different parts of a molecule, for instance, two metal centers, is referred to as a molecular wire. Thiazyl chains, that is, fragments of $(SN)_x$, could conveniently substitute the presently used molecular wires, typically polyacetylene fragments or fused aromatics.[2]

The appealing features of $(SN)_x$ stimulated a great interest in the study of its physical and structural properties and in the research of novel synthetic routes. Structure determinations indicated that the atoms of the polymer are linked together in an alternating cis−trans configuration[1,2] (which favors non-bonded S···N interactions), with bond angles at the sulfur and nitrogen atoms of about 106° and 120°, respectively. X-ray diffraction data[7−9] indicated that, in small oligomers, long (∼1.66 Å) and short (∼1.55 Å) S−N bonds are present, which is in line with a π system of the form N═S═N−S. Moreover, in some oligomers a (solid-state) configuration differing from the alternating cis−trans in the polymer was observed, where a cis arrangement is replaced by a trans one.[10,11]

The conducting properties of a polymer depend on quantities such as ionization energy (IE), electron affinity (EA), highest occupied molecular orbital−lowest unoccupied molecular orbital (HOMO−LUMO) energy gap, and valence bandwidth.[12] These quantities, in turn, are related to the electronic structure of the fragment precursors. Despite the interest in thiazyl chains, however, their electronic structure is almost unexplored. To our knowledge, only UV−vis absorption data are available in the literature,[2] where a red shift with increasing chain length was observed, as expected for a conjugated π system. IE data have been reported only for the cyclic dimer S_2N_2 and tetramer S_4N_4[13] but not for open thiazyl chains. The photoelectron spectrum[14] of solid-state $(SN)_x$ films was interpreted in terms of interchain interactions which increase the dimensionality of the film with a corresponding increase of the density of states near the Fermi level.

Over the past few years we have used a multidisciplinary approach based on photoelectron spectroscopy (PES), electron transmission spectroscopy (ETS), and theoretical calculations to characterize the electronic structures of the first oligomers of thiophene,[15] furan,[16] and methyl-,[17] methylchalcogeno-,[18] and carbonyl-substituted[19] thiophenes, extrapolating the results to predict the parameters of interest for the corresponding (ideal) gas-phase polymers.

In this paper, we apply the same approach to the gas-phase thiazyl chains R−NSN−R (**1**) and $(R-NSN)_2S$ (**2**), represented

* To whom correspondence should be addressed. Fax: ++39-051-2099456. E-mail: modelli@ciam.unibo.it.

10.1021/jp0025781 CCC: $20.00
Published on Web 12/05/2000

SCHEME 1

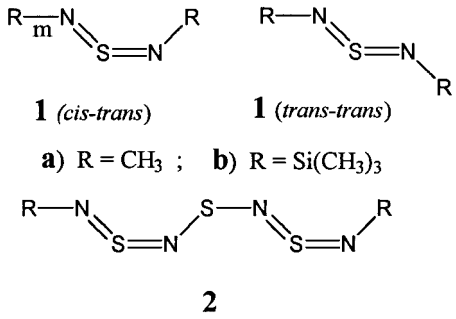

in Scheme 1, with the aims of characterizing their geometric and electronic structures and obtaining estimates for those of the polymer $(SN)_x$. The molecular orbital (MO) energies are computed for the neutral species with ab initio density functional theory (DFT) and semiempirical methods. The calculated MO eigenvalues are compared with the ionization energies (IEs) and the electron attachment energies (AEs, the negative of the EAs) measured in the PE and ET spectra of compounds **1b** and **2b**, where R = $Si(CH_3)_3$. The two techniques together give a complete picture of the frontier energy levels, although one of the major limits of ETS is that stable anion states (associated with positive EAs) cannot be observed.

An adequate theoretical approach for describing the energetics of temporary electron capture involves difficulties not encountered for cation states. In principle, the most correct approach is the calculation of the total electron scattering cross section with the use of continuum functions, although the evaluation of electron−molecule interactions is not easy.[20] In the Koopmans' theorem (KT) approximation,[21] the negatives of the energies of the filled and empty orbitals are assumed to equal the IEs and the EAs, respectively. This approximation neglects correlation and relaxation effects, which tend to cancel out when IEs, but not EAs, are evaluated. For this reason, KT predictions generally underestimate the latter by several electronvolts. The LUMO eigenvalues determined with Hartree−Fock (HF)/6-31G* calculations, however, were found[22] to correctly parallel the experimental AE trends in homologous compounds. In agreement, we have recently found that the HF/6-31G** eigenvalues satisfactorily parallel the experimental π^* AE trends in a series of π molecular systems.[23−25] In addition, we employ here more sophisticated methods, which account for correlation using the coupled-cluster theory,[26] for calculating the absolute value of the first vertical EA of H−NSN−H and CH_3−NSN−CH_3.

Experimental Section

PE Spectra. The He(I) spectra were recorded on a Perkin-Elmer PS-18 photoelectron spectrometer connected to a Datalab DL4000 signal analysis system. The bands, calibrated against rare-gas lines, were located using the position of their maxima, which were taken as corresponding to the vertical IEs. The accuracy of the IE values was estimated to be ±0.05 eV for peak maxima and ±0.1 eV for shoulders.

ET Spectra. Our ET apparatus is in the format devised by Sanche and Schulz[27] and has been previously described.[28] To enhance the visibility of the sharp resonance structures, the impact energy of the electron beam is modulated with a small ac voltage, and the derivative of the electron current transmitted through the gas sample is measured directly by a synchronous lock-in amplifier. The present spectra have been obtained by using the apparatus in the "high-rejection" mode[29] and are, therefore, related to the nearly total scattering cross section. The midpoint between the maximum and minimum of the derivatized signal has been taken as the most probable vertical AE (VAE). The electron beam resolution was about 50 meV (full width at half-maximum (fwhm)). The energy scales were calibrated with reference to the $(1s^12s^2)^2S$ anion state of He. Because of the broadness of the signals, the estimated accuracy is ±0.1 eV.

Synthesis. 1,3-Bis(trimethylsilyl)-1,3-diaza-2-thia-1,2-propadiene (**1b**) was synthesized following a reported procedure[30] and partly used to prepare 1,7-bis(trimethylsilyl)-1,3,5,7-tetraaza-2,4,6-trithia-1,2,5,6-heptatetraene (**2b**) according to the literature.[31]

Calculations. The geometries of molecules **1** and **2** (R = H, CH_3, and $Si(CH_3)_3$) were calculated by optimization with density functional methods at the B3LYP/6-31G* level. Each possible combination of a cis−trans configuration in the SN chain was constrained in the optimization to select the most stable structures as displayed in Scheme 1.

To achieve extrapolation to the polymers, *trans*-oligoethenes $H(CH{=}CH)_xH$ (with $x = 1-4$ and 10) and the model system $H_2(NSN)_5S_4$ with alternating cis−trans SN bonds were considered. The geometries of these molecules were optimized with several semiempirical methods (MNDO, AM1, PM3, and MINDO/3). Only the AM1 method gave bond angles and lengths in agreement with the experimental X-ray diffraction data for the $(SN)_x$ polymer.[2]

IEs and VAEs were evaluated by means of HF/6-31G* and AM1 calculations, within the KT approximation, and also by means of the DFT using the orbital energies of the transition state (TS) electronic configuration. At variance with the HF−KT approximation, with this approach both relaxation and correlation effects are taken in to account. DFT−TS calculations were performed with the ADF program[32] (version 1.1.3) using the VWN potential[33] for the LDA part and the gradient corrections of Becke[34] and Perdew[35] for the exchange and correlation potentials, respectively. All calculations with the ADF program employed a frozen core triple-ζ basis set with polarization functions.

Post-HF methods were used to calculate the first vertical electron affinity (VEA) of the smaller molecules **1a** (in the trans−trans and cis−trans configurations) and H−NSN−H (in the cis−trans configuration). Because the many-body perturbation theory (MBPT) seems to be not very reliable in EA calculations,[36] infinite-order coupled-cluster expansion was employed, that is, coupled cluster with all single and double substitutions (CCSD).[37] As implemented in the Gaussian 98 set of programs,[38] the CCSD calculations supply also the Möller−Plesset energies at the MP2, MP3, and MP4SDQ levels. In all of the post-HF calculations, the 6-31+G* basis set was used to account for the spatial diffuseness of the anionic states.

All of the semiempirical, HF, and post-HF calculations and DFT geometry optimizations were performed with the Gaussian 98 set of programs. The computer used was a conventional PC with a Pentium II processor.

Results and Discussion

The NSN group is a three-center four-electron π system, to which each nitrogen and sulfur atom contributes one and two electrons, respectively. Therefore, in compound **1**, the two lowest-lying (allylic) π_1 and π_2 MOs (sketched in Scheme 2) are completely filled, whereas the totally antibonding π_3^* is empty. The π system of **2** possesses five filled π MOs and two empty π^* MOs, which arise from the six in-phase or out-of-phase combinations between the allylic π orbitals of the two

SCHEME 2

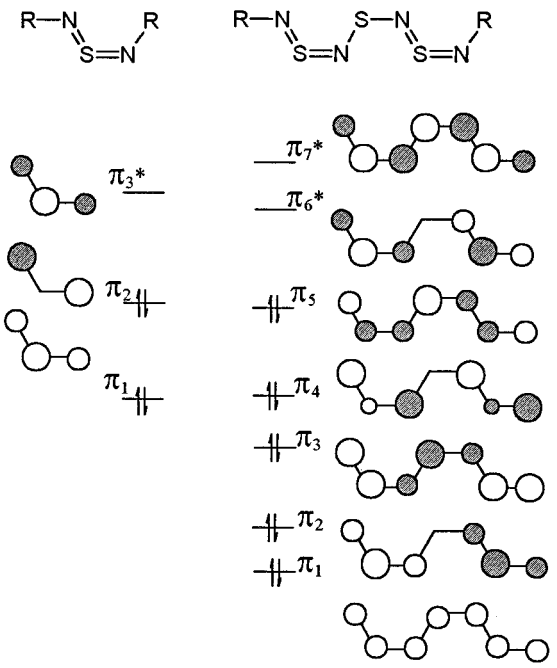

NSN groups and from the π lone pair orbital of the central sulfur atom (IE = 10.47 eV in H_2S[39] and 8.71 eV in $(CH_3)_2S$[40]). A qualitative representation (based on the wave function coefficients supplied by DFT calculations on $(HNSN)_2S$) is given in Scheme 2.

In general, an $(SN)_x$ (with x = even integer) polymer possesses $3x$ π electrons, which fill $^3/_4$ of the $2x$ π MOs. At variance with polyacetylene $(CH{=}CH)_x$ chains, where only the x bonding π MOs are occupied, in $(SN)_x$ chains, half of the antibonding π MOs are also occupied. This leads to an energy increase (IE decrease) of the HOMO and to a higher density of states in the valence band.

Although the representation of the $-S_2N_2-$ unit supplied by the structural formula $-N{=}S{=}N-S-$ is only an approximation, according to the X-ray structure analysis of $R(N{=}S{=}N-S)_2R$ and $RN{=}S{=}N-S-N{=}S{=}N-SR$,[8,9] the SN distances represented with double and single bonds are significantly different (about 1.56 and 1.65 Å, respectively), the configuration being planar with alternating cis and trans arrangements.

The geometries calculated here for molecules **1a**, **1b**, **2a**, and **2b**, optimized at the B3LYP/6-31G* level, are in good agreement with the above experimental data. There are two possible isomers for R—N=S=N—R, which differ in the arrangement of the R substituents. The isomer labeled cis−trans in Scheme 1 is calculated to be more stable (about 5 kcal mol^{-1}) than the trans−trans isomer. This result is in line with a larger (repulsive) interaction between the two nitrogen lone pair orbitals (σ_n) in the latter. In agreement, according to the HF/6-31G* calculations, the energy splitting between the two MOs with mainly σ_n character is 0.45 eV in cis−trans **1b** (see Table 1) and 1.00 eV in trans−trans **1b** (not reported). The corresponding most stable isomer predicted for molecule **2** is like the one sketched in Scheme 1 and in Figure 1. The latter represents the (planar) most stable conformer of **2a** together with the calculated bond lengths, whereas the calculated bond angles are 117° at N(1), 109.9° at S(2), 118.9° at N(3), 103.7° at S(4), 125.5° at N(5), 112.1° at S(6), and 120.8° at N(7).

Figure 2 reports the potential energy curve obtained with B3LYP/6-31G* calculations as a function of the torsional angle (θ) around a single SN bond in $(HNSN)_2S$, reoptimizing the

TABLE 1: Orbital Energies (eV) of the Neutral Molecules Obtained with ab Initio (HF/6-31G*) and Semiempirical (AM1) Calculations and Orbital Eigenvalues for the Electronic Configuration of the TS Obtained with DFT−TS Calculations

	orbital symmetry (C_s)	HF/6-31G*	DFT−TS	AM1
1a cis−trans	a′	6.13	1.98	2.30
	a′	5.41	1.54	1.39
	a″ (π_3*)	1.57	0.39	−1.23
	a″ (π_2)	−9.06	−9.26	−8.87
	a′ (σ_n)	−11.11	−9.82	−10.56
	a′ (σ_n)	−11.88	−10.66	−11.27
	a″ (π_1)	−13.41	−11.94	−12.35
	a′ (σ_{CH})	−14.38	−12.46	−13.63
1b cis−trans	a′	5.42	1.39	1.33
	a′	5.16	1.02	0.85
	a″ (π_3*)	1.19	−0.22	−1.11
	a″ (π_2)	−9.57	−8.63	−9.07
	a′ (σ_n)	−10.39	−8.58	−9.71
	a′ (σ_n)	−10.84	−8.95	−10.13
	a″ (σ_{SiC})	−11.58	−9.45	−10.92
	a′ (σ_{SiC})	−11.91	−9.50	−11.10
	a″ (σ_{SiC})	−12.10	−10.29	−11.44
	a′ (σ_{SiC})	−12.15	−10.24	−11.33
	a″ (σ_{CH})	−14.19	−11.01	−12.87
	a′ (σ_{CH})	−14.27	−11.23	−12.76
	a″ (π_1)	−14.30	−11.34	−14.41
2a	a′	4.06	0.93	0.50
	a″ (π_7*)	1.63	−0.24	−1.23
	a″ (π_6*)	0.35	−1.19	−1.88
	a″ (π_5)	−7.57	−7.62	−8.01
	a″ (π_4)	−9.92	−9.06	−9.64
	a′ (σ_n)	−11.03	−9.11	−10.57
	a′ (σ_n)	−11.84	−9.70	−11.13
	a″ (π_3)	−11.98	−10.37	−11.14
	a′	−12.00	−10.10	−11.28
	a′	−12.67	−10.80	−11.89
	a″ (π_2)	−14.27	−11.88	−13.05
	a′ (σ_{CH})	−14.75	−12.13	−13.81
	a′ (σ_{CH})	−15.39		−13.93
	a″ (π_1)	−15.44	−12.70	−13.87
2b	a′	4.20	0.82	0.48
	a″ (π_7*)	1.49	−0.44	−1.11
	a″ (π_6*)	0.24	−1.39	−1.77
	a″ (π_5)	−7.77	−7.44	−7.96
	a″ (π_4)	−10.18	−8.59	−9.66
	a′ (σ_n)	−10.58	−8.27	−9.83
	a′ (σ_n)	−10.89	−8.65	−10.16
	a″ (σ_{SiC})	−11.47	−9.16	−10.78
	a′ (σ_{SiC})	−11.50	−9.06	−10.78
	a″ (σ_{SiC})	−12.03	−9.77	−11.33
	a′ (σ_{SiC})	−12.17	−9.47	−11.26
	a′ (σ_{SN})	−12.52	−9.76	−11.66
	a′ (σ_{SN})	−12.62	−10.18	−11.73
	a″ (π_3)	−12.87	−10.51	−11.88
	a″ (σ_{CH})	−14.21	−11.06	−12.89
H−NSN−H	a′	5.11	1.80	1.66
	a″ (π_3*)	1.26	0.16	−1.36
	a″ (π_2)	−9.91	−10.78	−9.59
	a′ (σ_n)	−11.96	−11.32	−11.21
	a″ (π_1)	−15.07	−14.41	−14.14
$H_2(NSN)_5S_4$	a′	3.81	−0.25	−0.12
	a″ (π_{19}*)	1.87	−1.02	−1.04
	a″ (π_{18}*)	1.52	−1.30	−1.32
	a″ (π_{17}*)	0.94	−1.68	−1.60
	a″ (π_{16}*)	0.17	−2.17	−1.98
	a″ (π_{15}*)	−0.59	−2.64	−2.40
	a″ (π_{14})	−6.68	−6.45	−7.43
	a″ (π_{13})	−7.60	−7.01	−8.03
	a″ (π_{12})	−8.67	−7.64	−8.75
	a″ (π_{11})	−9.76	−8.32	−9.52
	a″ (π_{10})	−11.17	−9.18	−10.51
	a′ (σ_n)	−11.25	−8.64	−10.53

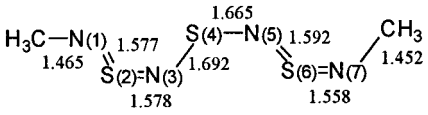

Figure 1. Calculated (B3LYP/6-31G*) geometry for **2a**.

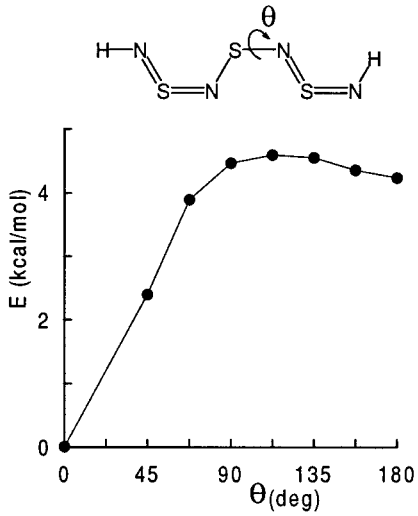

Figure 2. B3LYP/6-31G* potential energy curve as a function of the torsional angle (θ) around the central SN bond in $(HNSN)_2S$ with reoptimization of the other geometrical parameters.

other geometrical parameters. These results do not support a reasonable a priori expectation of an energy maximum for $\theta = 90°$ (reduced conjugation of the π system) followed by a nearly symmetric energy decrease from $\theta = 90°$ to $\theta = 180°$. On the contrary, the energy of the opposite planar conformer ($\theta = 180°$) is only slightly smaller than that of the perpendicular rotamer. According to the more accurate set of calculations (which accounts for geometrical rearrangements as a function of θ), the barrier to rotation is 4.59 kcal/mol, and the energy remains nearly constant from $\theta = 90°$ to $\theta = 180°$. As a tentative explanation, it can be noticed that (i) electron occupation of the strongly S−N antibonding HOMO (π_5, see Scheme 2) reduces the stabilizing effect of the conjugation; (ii) in the $\theta = 180°$ conformer, one of the two intramolecular attractive $S^{\delta+}\cdots N^{\delta-}$ 1,4 interactions present in the $\theta = 0°$ conformer is strongly reduced; and (iii) in the $\theta = 180°$conformer the σ lone pairs of N(3) and N(5) give rise to the repulsive interaction mentioned above for the trans−trans isomer of **1**.

Analysis of the Mulliken populations obtained with B3LYP/6-31G* calculations in $(HNSN)_2S$ is consistent with the above hypothesis, with the charges predicted at the nitrogen and sulfur atoms being rather high: N(1), −0.70; S(2), +0.65; N(3), −0.59; S(4), +0.55; N(5), −0.59; S(6), +0.68; and N(7), −0.65. The calculated charges depend only slightly upon the conformation.

IEs. The sulfur−nitrogen chains **1** and **2** can be prepared[30,31] as stable compounds when $R = Si(CH_3)_3$. Figure 3 reports the PE spectra of the trimethylsilyl derivatives **1b** and **2b**, in the 6−18 eV energy range. The spectrum of **1b** displays two rather broad bands, peaking at 9.15 and 10.8 eV, followed by a large unresolved envelope of signals starting above 12 eV, in the energy range where ionization from the σ_{CH} MOs typically occurs.

The large widths of the first two bands of the spectrum suggest that both are due to several unresolved ionization events. The three outermost filled MOs of **1b** are expected to be the π_2 MO (see Scheme 1) and the two σ MOs (σ_n) originating from the nonbonding nitrogen lone pairs (IE = 10.15 eV in NH_3[39]).

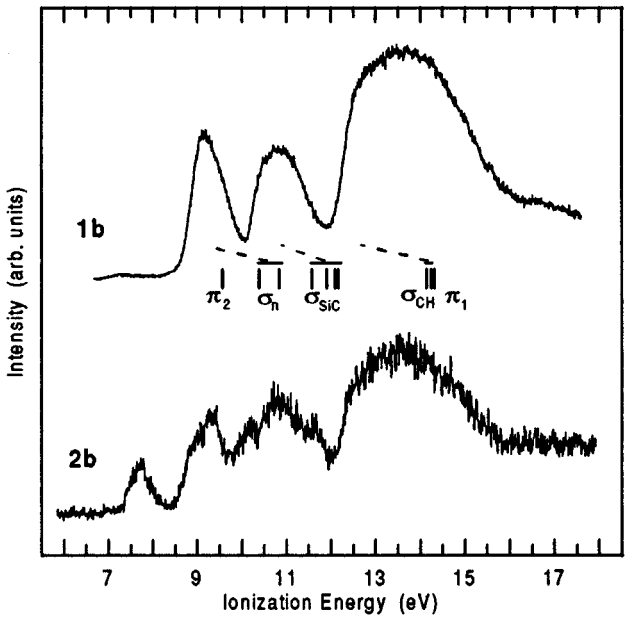

Figure 3. He I photoelectron spectra of **1b** and **2b**. The IEs supplied by KT−HF/6-31G* calculations for **1b** are also reported.

Moreover, ionization from the higher-lying σ MOs with mainly Si−C character (σ_{SiC}) is known to peak in the 10.7−11.0 eV energy range in hexamethyldisilane.[41] The corresponding signals in the PE spectrum of **1b** should thus contribute to the broad second band (centered at 10.8 eV).

Table 1 reports the filled and empty orbital energies of the neutral states of molecules **1a,b** and **2a,b** obtained with ab initio HF/6-31G* and semiempirical AM1 calculations and the orbital eigenvalues for the electronic configuration of the TS obtained with DFT calculations. The latter method accounts for relaxation effects in the final state, so that the calculated orbital eigenvalues constitute an approximation to the ion/neutral-state energy difference. All three sets of theoretical results for **1b** confirm the above qualitative prediction of the energy ordering of the outermost filled orbitals: at higher energy (lower IE) the π_2 MO and the two σ_n MOs, then four σ MOs (closely spaced in energy) with mainly Si−C character, and at sizeably lower energy the onset of the σ_{CH} orbitals. However, except for the π_2 MO, the calculated values do not match the measured IEs, as shown in Figure 3, where the HF/6-31G* MO energies are directly compared with the spectrum.

HF calculations neglect correlation and relaxation effects. The two approximations tend to compensate when IEs are evaluated. As a result, π IEs are usually reproduced satisfactorily. Because of significantly different relaxation effects, however, the agreement worsens when σ MOs, in particular localized lone pairs, are involved.[18,19,23] As a test, we carried out HF/6-31G* calculations on benzaldehyde. The first two π IEs (9.59 and 9.81 eV[42]) are reproduced within ±0.1 eV, whereas the energy obtained for the σ oxygen lone pair (−11.46 eV) overestimates the experimental IE (9.6 eV[42]) by almost 2 eV.

Once the overestimation of the calculated σ IEs is accounted for, the first band of the spectrum of **1b** is associated with three unresolved contributions (from π_2 and the two σ_n MOs) and the second band with four σ_{SiC} MOs (as shown in Figure 3), in agreement with their relative intensities. It can be noticed that only the DFT−TS results (although underestimating the values) are successful in predicting the first three IEs very close to each other, with the ordering $\sigma_n < \pi_2 < \sigma_n$.

The PE spectrum of the trimethylsilyl-substituted seven-membered π system **2b** (see Figure 3) displays a single peak at

low IE (7.75 eV), followed by partially overlapping signals which give rise to a shoulder at 8.9 eV and maxima at 9.3, 10.2, 10.8, and 11.7 eV. All three sets of theoretical results predict (i) the HOMO to be the π_5 MO (see Scheme 2), with large central sulfur atom character; (ii) two outermost σ_n MOs split in energy by 0.3−0.4 eV; and (iii) a group of four σ_{SiC} MOs close in energy.

The HF/6-31G* calculations reproduce exactly the first experimental IE, associated with the π_5 MO. It can also be noticed that the stabilization of the π HOMO predicted by the calculations upon replacement of methyl groups with silyl groups (in both compounds **1** and **2**) is in line with the IE shift experimentally observed in benzene[43] and ethene[44] derivatives. According to the same calculations, ionization from the second π orbital occurs at 10.18 eV. We therefore assign the maximum at 10.2 eV in the spectrum to the π_4 MO. The shoulder at 8.9 eV and the maximum at 9.3 eV are assigned to σ_n MOs. As found for **1b**, the absolute IE values of the σ MOs are overestimated by more than 1 eV by the HF/6-31G* calculations. The broad maximum at 10.8 eV is thus assigned to the four σ_{SiC} MOs, and the following maximum at 11.7 eV is assigned to the two nearly degenerate σ MOs of mainly SN character, as indicated by the calculations. Finally, the signal from the π_3 MO should fall at the onset (∼12.5 eV) of the broad envelope associated with the innermost σ MOs.

It should be noted that the DFT−TS results are in better agreement with the experiment as far as the relative σ and π MO energies are concerned but fail to reproduce the absolute IE values which are predicted to be too low. Moreover, this discrepancy increases with increasing IE, so that the DFT calculations supply a filled level structure which is compressed toward the HOMO.

The present findings show quite a low IE from the outermost π MO of the NSN fragment (the corresponding π_2 IE of the NO_2 group, which is an analogous three-center four-electron π system, is about 2 eV higher[45]). In $(SN)_x$ chains, the NSN fragments alternate with sulfur atoms. Because of the low IE of the S lone pairs and strong lone pair/π_{NSN} mixing, the first IE decreases rapidly upon chain formation, as demonstrated by the PE spectrum of **2b** and by calculations.

EAs. ETS is one of the most suitable means for measuring the energies of electron attachment to gas-phase samples. This technique takes advantage of the sharp variations in the total electron−molecule scattering cross section caused by resonance processes, namely, temporary capture of electrons into empty MOs. Because this process is rapid relative to the time scale of nuclear motion, temporary anions are formed at the equilibrium geometry of the neutral molecule. The measured VAEs are thus the negative of the VEAs, thus providing electronic structure data complementary to the IEs supplied by PES.

The ET spectra of compounds **1b** and **2b** in the 0−6 eV energy range are reported in Figure 4. The spectrum of **1b** displays a broad (fwhm = 1.2 eV) resonance centered at 2.8 eV and an even broader and weaker resonance at 4.5 eV. Electron capture into the lowest σ^*_{SiC} MOs was found[28] to give rise to a broad resonance above 3 eV in the trimethylsilyl derivatives of both ethene and benzene. Thus, the first resonance of **1b** can be reasonably associated with σ^*_{SiC} MOs, stabilized by mixing with higher-lying σ^* MOs of the NSN skeleton. This assignment implies that the anion state associated with the LUMO (π^*_3) must lie close to zero energy (where resonances are hidden by the intense electron beam signal) or below zero energy (that is, the π^* anion state is stable with respect to the neutral molecule and cannot be observed by ETS). In line with

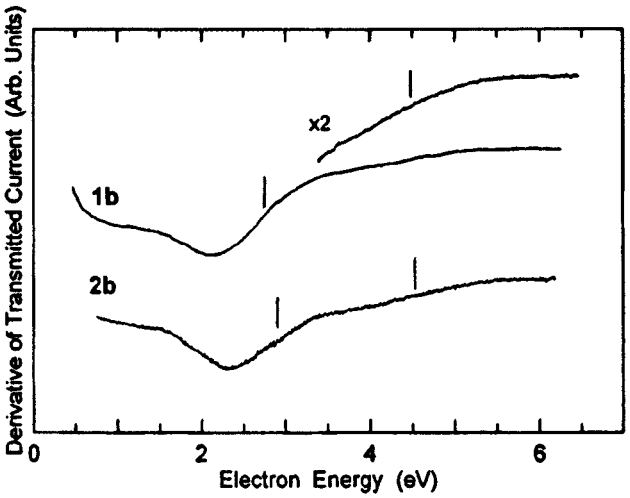

Figure 4. Derivative of the electron current transmitted through gas-phase **1b** and **2b**, as a function of the incident electron energy. Vertical lines locate the most probable VAEs.

the assignment of the first feature in the spectrum of **1b** to σ^*_{SiC} MOs, the spectrum of **2b** is quite similar, the measured VAEs (2.9 and 4.6 eV) being equal to those of **1b** within experimental error. In this case, both the LUMO and second LUMO, the π^*_6 and π^*_7 MOs, must lie close to or below zero energy.

As mentioned in the Introduction, the empty orbital energies supplied by KT−HF/6-31G* calculations have been found to reproduce the experimental trends of the vertical π^* VAEs observed in series of analogous molecules, but the absolute values are systematically too high (often by more than 2 eV). Moreover, the discrepancy tends to increase with increasing energy. As far as the DFT−TS calculations are concerned, the lack of literature data does not allow an estimate of their reliability in reproducing VAEs. Thus, only the trends of the empty MO energies reported in Table 1 can be considered.

Both the HF/6-31G* and the DFT−TS calculations predict a stabilization (0.5 ± 0.1 eV) of the π^*_3 LUMO on going from **1a** to **1b** and a stabilization of both of the two empty π^* MOs on going from **2a** to **2b**, that is, upon replacement of methyl groups with trimethylsilyl groups. In agreement with this prediction, the stabilizing effect of the trimethylsilyl group, ascribed to π^*/σ^*_{SiC} mixing, has been observed in the ET spectra of the ethene,[28] benzene,[28] and diimine[24] derivatives.

The most significant result of the calculations relates to the (not obvious) energy evolution of the empty π^* MOs on going from **1** to **2** (with either methyl or silyl substituents). The two π^* MOs of butadiene are almost symmetrically split with respect to the π^* MO of ethene, as shown by the ET spectra[46] and in agreement with the present (not reported) calculations. In contrast, at all three levels of theory, the π_6^* and π_7^* MOs of **2** are predicted to be respectively sizably more stable and about as stable as the π_3^* MO of **1** (see Table 1).

The two empty π^* MOs of **2** arise from the out-of-phase and in-phase combinations of the π_3^* MO of the NSN fragments (see Scheme 2). For symmetry reasons, the former cannot mix with the lone pair of the central sulfur atom (and should thus be nearly unperturbed in energy), whereas the latter mixes with (and is destabilized by) the S lone pair. Many ETS data[47] have shown that oxygen or nitrogen atoms adjacent to a π system cause a sizable destabilization of the empty π^* MOs of proper symmetry, because of the charge-transfer lone pair/π^* interaction. However, when the substituent is a sulfur atom, this destabilization is not observed. MS-Xα calculations repro-

TABLE 2: Energy Difference (eV) between the First Anion State (at the Equilibrium Geometry of the Neutral State) and the Neutral Molecule Calculated at Different Levels of Theory with the 6-31+G* Basis Set[a]

	HF (no correl.)	MP2	MP3	MP4−SDQ	CCSD	DFT−TS
1a trans−trans	−0.350	+0.288	−0.033	+0.039	−0.026	−0.024
1a cis−trans	+0.053	+0.704	+0.370	+0.443	+0.370	+0.390
H−NSN−H cis−trans	−0.207	+0.370	+0.131	+0.179	+0.125	+0.162

[a] The DFT−TS eigenvalues are also reported for comparison.

duced[48] the experimental data and ascribed the peculiar behavior of sulfur to the mixing of the π^* MOs with S_{3d} orbitals, which counteracts the effect of the lone pair/π^* interaction. In agreement, replacement of a CH_2 group with a sulfur atom in dicarbonyl derivatives was found[49] to cause a stabilization of empty π^* MOs which cannot mix with the S lone pair for symmetry reasons (but can mix with suitable S_{3d} orbitals). On this basis, the π_6^* and π_7^* MOs of **2** are expected to lie at lower and nearly equal energy, respectively, with respect to the π_3^* MO of **1**. This expectation is fully confirmed by the present calculations, according to which, however, the S_{3d} orbital contribution to the π^* MOs is small.

To obtain a reliable evaluation of the absolute VEA values, we carried out post-HF calculations which employ infinite-order CCSD on both isomers of $CH_3-NSN-CH_3$ and on the most stable (cis−trans) isomer of H−NSN−H. The calculations, which include correlation effects, were performed on the π anion state (at the geometry of the neutral) and on the neutral state, thus also accounting for relaxation effects. The same method supplied a VAE of 0.52 eV for nitromethane, in excellent agreement with the resonance observed at 0.45 eV in its ET spectrum.[50]

The CCSD results are reported in Table 2, together with those supplied by standard post-HF methods (MP2, MP3, and MP4) and by HF calculations. The reported values are the energy difference between the anion and the neutral state (at the equilibrium geometry of the latter) and thus represent the first VAE (that is, the negative of the first VEA). The DFT−TS eigenvalues are also included in Table 2 for comparison. The CCSD calculations predict the π^* VAE of the cis−trans isomer of **1a** to be −0.37 eV, whereas a slightly positive (0.026 eV) VEA is calculated for the (less stable) trans−trans isomer. The 0.4 eV higher EA of the trans−trans isomer is reproduced at all levels of theory, including the KT−HF calculations, according to which the LUMO energy is 1.17 eV (not reported in Table 1) and 1.57 eV for the trans−trans and cis−trans isomers, respectively. On going from **1a** to H−NSN−H, all of the calculations predict an EA increase of ∼0.25 eV, which is in good agreement with the VAE shift observed in the ET spectra of small methyl-substituted π systems.[46] A comparison of the CCSD results with the other data of Table 2 shows that (i) quite similar VAEs are obtained from the MP4 and MP3 calculations; (ii) the MP2 calculations overestimate the VAEs by ∼0.3 eV; and (iii) the HF calculations (which neglect correlation) tend to underestimate (∼0.3 eV) the VAEs. Most importantly, as far as the applicability of the calculations to larger molecular systems is concerned, the last column of Table 2 shows that the eigenvalues provided by the TS−DFT method are equal (within 0.04 eV) to the CCSD VAEs.

The VAEs supplied by the CCSD calculations for **1a** and H−NSN−H (0.370 and 0.125 eV, respectively) are consistent with the absence of π^* resonances in the ET spectra of **1b** and **2b**. Once the above-mentioned stabilizing effect of the trimethylsilyl substituents is considered, the π anion state of **1b** is easily predicted to lie a few tenths of an electronvolt below zero energy (i.e., **1b** possesses a positive EA), which is in line with the DFT−TS eigenvalue (−0.22 eV; see Table 1). Thus, according to the theoretical results of Table 1, even the highest π anion state of **2b** must be slightly stable, whereas the first anion state is much more stable. In particular, the DFT−TS calculations evaluate the VEAs associated with electron addition to π_6^* and π_7^* to be 1.39 and 0.44 eV, respectively.

TABLE 3: Experimental and Calculated First IE and VAE (eV) for *trans*-H(CH=CH)$_x$H and for (NSN)$_5$S$_4$H$_2$[a]

	trans-H(CH=CH)$_x$H, where x =						
	1	2	3	4	10	∞	$H_2(NSN)_5S_4$
				IE			
expt	10.51	9.03	8.29	7.79			
Hückel	10.56	8.92	8.24	7.90	7.41	7.28	
AM1	10.55	9.33	8.75	8.42	7.83		7.43
HF/6-31G*							6.68
extrapolation (expt/AM1)					7.42		6.93
				VAE			
expt	1.73	0.62	∼0				
Hückel	1.8	0.60	0.1		−0.50	−0.60	
DFT−TS							−2.64

[a] Expt IEs taken from refs 52 and 53 and expt VAEs from ref 46.

The present results demonstrate that the electron-acceptor properties of H−NSN−H not only are sizeably larger than those of ethene (VAE = 1.73 eV[51]), that is, the repeating unit of polyacetylene, but are even larger than those of the prototype electron acceptor, the $-NO_2$ group (compare with the experimental and CCSD VAEs of CH_3-NO_2, quoted above). Moreover, as mentioned in the preceding section, the NSN π system simultaneously possesses much greater electron-donor properties. Although in $(SN)_x$ chains the π_3^* MOs of the NSN fragments interact through sulfur atoms (which do not possess empty π^* orbitals), the present calculations on **2** indicate that the EA of the first oligomers rapidly increases with the chain length. On the basis of these findings, therefore, strong electron-acceptor properties can be foreseen for $(SN)_x$.

Extrapolation to the Polymer. Only three π IE values are supplied by the PE spectra of molecules **1b** and **2b**. In addition, the unresolved contribution of the π_2 MO of **1b** to the first band of the spectrum cannot be quoted with accuracy (we assume the π_2 IE to be 9.35 eV, midway between the peak of the band and the value supplied by the HF/6-31G* calculations). To build a calibration curve between experimental and calculated IEs based on a larger set of data, we include also the experimental HOMO IEs of the *trans*-oligoethenes H(CH=CH)$_x$H, with x = 1−4, available in the literature.[52,53] This also allows for a comparison of the extrapolated IE of $(SN)_x$ with that of polyacetylene. Table 3 reports the first IE obtained with semiempirical AM1 calculations for the ethene oligomers, with x = 1−4 and 10, and for $H_2(NSN)_5S_4$ (which possesses a number of heteroatoms close to the number of carbon atoms of the ethene decamer).

The seven experimental π IEs are plotted versus the corresponding AM1 values in Figure 5. A rather good linear fit is

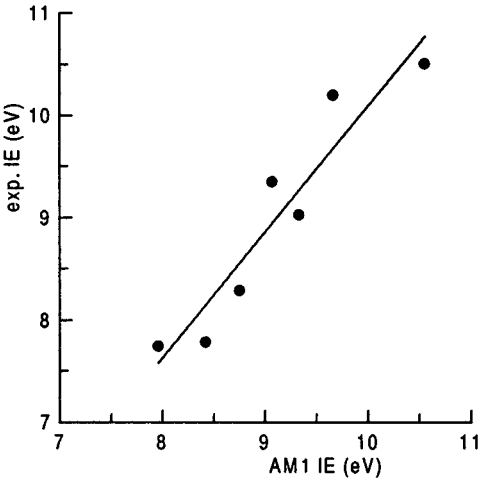

Figure 5. Diagram of the experimental π IEs of **1b** and **2b** and of the HOMO IE of the *trans*-oligoethenes $H(CH{=}CH)_xH$, with $x = 1-4$, versus the corresponding values supplied by AM1 calculations.

found, according to which the experimental and calculated IEs are related by eq 1:

$$IE_{exp} = 1.23IE_{AM1} - 2.21 \quad (1)$$

When the IE values calculated for $H(CH{=}CH)_{10}H$ (7.83 eV) and $H_2(NSN)_5S_4$ (7.43 eV) are introduced in eq 1, the (extrapolated) experimental values of 7.42 and 6.93 eV, respectively, are obtained. A different approach can be used for extrapolating the first IE of the ethene decamer. According to the Hückel method, which can accurately reproduce IE values when parametrized with experimental data, the energy of the outermost π MO arising from the interaction among x equal atomic (or group) orbitals with a linear topology is given by the simple relation

$$E = \alpha + 2\beta \cos(x\pi/(x+1)) \quad (2)$$

where α (the Coulomb integral) is the energy of each orbital before interaction and β (the resonance integral) reflects the extent of interaction. A plot of the negative of the first experimental IE of $H(CH{=}CH)_xH$ ($x = 1-4$) versus $\cos(x\pi/(x+1))$ gives a good linear correlation, from which $\alpha = -10.56$ and $\beta = -1.64$ can be obtained. With these parameters, eq 2 can be used for evaluating the first IE as a function of x (see Table 3). For $x = 10$, the calculated IE (7.41 eV) coincides with the value (7.42 eV) obtained by extrapolating the expt/AM1 fitting, confirming its reliability.

As a further attempt to confirm the extrapolated IE (6.93 eV) for $H_2(NSN)_5S_4$, we also performed on this molecule (with the geometry optimized at the AM1 level) HF/6-31G* calculations, which closely reproduce the π IEs measured in **1b** and **2b**. The first IE (6.68 eV; see Table 1) is predicted to be about 0.2 eV lower than the extrapolated value.

Equation 2 predicts the IE of the $(CH{=}CH)_x$ polymer ($x =$ infinite) to be 7.28 eV, namely, ~0.1 eV smaller than that of the decamer. Thus, under the assumption that the IE of $H_2(NSN)_5S_4$ is 6.8 eV (average between the extrapolated and the HF/6-31G* values), the first IE of the $(SN)_x$ polymer is evaluated to be ~6.7 eV, that is, 0.6 eV smaller than that of polyacetylene and slightly smaller than that of polythiophene (6.9 eV[15]). The first main ionization band displayed in the solid-state PE spectrum[14] of the $(SN)_x$ polymer peaks at approximately 4.4 eV which, once solid-state relaxation energy (about 2 eV in *p*-terphenyl[54]) is taken into account, gives a value commensurate with our predicted value of 6.7 eV for the gas-phase polymer.

TABLE 4. Comparison of the First IE and VEA and of the HOMO−LUMO Energy Gap (eV) Estimated for Different (Ideal) Gas-Phase Polymers

	IE (eV)	VEA (eV)	$\Delta_{HOMO-LUMO}$ (eV)
polythiophene[16]	6.9	1.0	5.9
poly(thienylene ketone)[19]	9.1	2.7	6.4
trans-polyacetylene	7.3	0.6	6.7
$(SN)_x$	6.7	≥2	≤4.7

Evaluation of the VEA of the (ideal) gas-phase $(SN)_x$ polymer cannot rely on extrapolation of experimental data on small oligomers, which are inaccessible by ETS. As noticed above, the eigenvalues supplied by the DFT−TS calculations for the LUMO (π_3*) of H−NSN−H and of **1a** perfectly match the anion/neutral energy difference found with more sophisticated CCSD calculations. Although this is no guarantee that the calculated results are also reliable for larger molecular systems, we carried out DFT−TS calculations on $H_2(NSN)_5S_4$ (with the geometry optimized at the AM1 level). The first VEA is calculated to be +2.64 eV, and all of the five empty π* MOs are predicted to lie below zero energy and to be closely spaced in energy (see Table 1). In particular, according to the DFT results, the highest-lying π_{19}* MO is about 1.2 eV more stable with respect to the LUMO (π_3*) of H−NSN−H, which is at variance with the HF/6-31G* and AM1 calculations which predict the reverse energy ordering. This casts doubt upon the possibility that the DFT calculations can overestimate all of the π* VEAs of the larger molecule. At the HF/6-31G* level (see Table 1), the LUMO is stabilized by 1.85 eV on going from H−NSN−H to $H_2(NSN)_5S_4$. Subtraction of this energy shift to the VEA (−0.125 eV) predicted by the CCSD calculations for H−NSN−H gives a VEA (+1.73 eV) for $H_2(NSN)_5S_4$ sizably smaller than that predicted by the DFT−TS calculations. Even this estimate, however, leads to a large positive VEA (~2 eV) for the $(SN)_x$ polymer.

Regardless of its accurate determination, the high VEA of thiazyl chains is confirmed by the very small energy of the HOMO−LUMO transition (522 nm, 2.38 eV[2]) in $(Ar{-}NSN)_2S$, with $Ar = C_6H_5$, with the corresponding transition energy in the thiophene trimer (first IE = 7.43 eV) being 3.52 eV.[16]

An evaluation of the VEA of polyacetylene is easily obtained by the resonances observed in the ET spectra of ethene, *trans*-butadiene, and *trans*-hexatriene.[46] The measured VAEs (Table 3 reports only those associated with the LUMO) are nicely accounted for within a Hückel model (neglecting the filled MOs) using α ($\pi^*_{C=C}$) = 1.8 eV and $\beta = -1.2$ eV. These parameters lead to a positive VEA of 0.6 eV for the polymer. According to the present analysis, $(SN)_x$ would thus be not only a better electron donor but also a better electron acceptor than *trans*-polyacetylene.

Table 4 compares the first IE and VEA evaluated here for $(SN)_x$ and polyacetylene with those reported in the literature for polythiophene[16] (which presents good conductivity properties upon both positive and negative doping) and poly(thienylene ketone), an alternating sequence of thiophene rings and carbonyl groups with very high electron-acceptor properties. It can be noticed that $(SN)_x$ possesses the smallest IE and a high VEA, comparable to that of poly(thienylene ketone). As a result, the HOMO−LUMO energy gap (evaluated from the difference between the IE and EA values) in $(SN)_x$ is exceptionally small. The efficiency of $(SN)_x$ fragments as molecular wires is thus fully in line with the present study of the filled and empty level

structures, which also indicates that the $(SN)_x$ polymer should display better conductive properties than those of polyacetylene and polythiophene and be more suitable for both positive and negative doping.

Conclusions

The photoelectron spectra of **1b** and of **2b** are interpreted with the aid of ab initio HF/6-31G* and semiempirical AM1 calculations, at the KT level and using DFT−TS calculations. The results show that the first π IE of the N═S═N fragment is relatively low and that the IE rapidly decreases upon formation of $(SN)_x$ chains, where the π_{NSN} MOs mix with sulfur lone pair orbitals.

Extrapolation of the data leads to an IE of 6.7 eV for the (ideal) gas-phase $(SN)_x$ polymer, to be compared with the corresponding values of 6.9 and 7.3 eV for polythiophene and *trans*-polyacetylene, respectively.

The ET spectra of **1b** and **2b** do not display π^* resonances, indicating that the π^* anion state of the former and even the second π^* anion state of the latter either lie close to zero energy (where the spectral features can be hidden by the intense electron beam signal) or are stable with respect to the neutral molecule. In agreement, the VEA obtained with coupled-cluster calculations for H−NSN−H and CH_3−NSN−CH_3 is only slightly negative (about −0.1 eV). The DFT−TS eigenvalues closely match these results and predict the first and the second anion states of **2b** to be respectively largely stable and stable (in agreement with the ET spectrum) and also predict a very large positive VEA ($\geq$2.7 eV) for the $(SN)_x$ polymer. An evaluation of the polymer VEA based on KT−HF/6-31G* calculations leads to a somewhat smaller value (about 2 eV).

Although the absence of experimental values on the fragment molecules does not allow for an accurate extrapolation to the VEA of the polymer, the fact that even the smallest fragment (N═S═N) possesses a VEA close to zero (compare with −1.15 eV for thiophene and −1.73 eV for ethene) and the indications supplied by the calculations do not leave any doubts about a sizeably larger VEA of the $(SN)_x$ polymer with respect to *trans*-polyacetylene and polythiophene. With respect to these polymers, $(SN)_x$ is thus a better electron donor and a better electron acceptor at one and the same time, which is in line with its peculiar electron conducting properties.

Acknowledgment. The authors thank the Italian Ministero dell'Università e della Ricerca Scientifica e Tecnologica for financial support. The technical assistance of Mr. G. Bragaglia is also acknowledged.

References and Notes

(1) Labes, M. M.; Love, P.; Nichols, L. F. *Chem. Rev.* **1979**, *79*, 1.
(2) Rawson, J. M.; Longridge, J. J. *Chem. Soc. Rev.* **1997**, *26*, 53.
(3) Smart, L.; Moore, E. *Solid State Chemistry*: *An Introduction*; Chapman and Hall: London, 1992.
(4) Cohen, M. J.; Harris, J. S. *Appl. Phys. Lett.* **1978**, *33*, 812.
(5) In *Handbook of Conducting Polymers*; Skotheim, T. A., Ed.; Marcel Dekker: New York, 1986; Vol. 1.
(6) Ward, M. D. *Chem. Soc. Rev.* **1995**, *24*, 121.
(7) Bestari, K.; Oakley, R. T.; Cordes, A. W. *Can. J. Chem.* **1991**, *69*, 94.
(8) Zibarev, A. V.; Gatilov, Y. V.; Bagrianska, I. Yu.; Konchenko, S. N. *Polyhedron* **1992**, *21*, 2787.
(9) Zibarev, A. V.; Miller, A. O.; Gatilov, Y. V.; Furin, G. G. *Heteroat. Chem.* **1990**, *6*, 443.
(10) Mayerle, J. J.; Kuyper, J.; Street, G. B. *Inorg. Chem.* **1978**, *17*, 2610.
(11) Isenberg, W.; Mews, R.; Sheldrick, G. M. *Z. Anorg. Allg. Chem.* **1985**, *525*, 54.
(12) Brédas, J. L.; Thémans, B.; Fripiat, J. G.; André, J. M.; Chance, R. R. *Phys. Rev. B*: *Condens. Matter* **1984**, *29*, 6761.
(13) Findlay, R. H.; Palmer, M. H.; Downs, A. J.; Edgell, R. G.; Evans, R. *Inorg. Chem.* **1980**, *19*, 1307.
(14) Kelemen, S. R.; Herschbach, D. R. *J. Chem. Phys.* **1982**, *86*, 4388.
(15) Jones, D.; Guerra, M.; Favaretto, L.; Modelli, A.; Fabrizio, M.; Distefano, G. *J. Phys. Chem.* **1990**, *94*, 5761.
(16) Distefano, G.; Jones, D.; Guerra, M.; Favaretto, L.; Modelli, A.; Mengoli, G. *J. Phys. Chem.* **1991**, *95*, 5761.
(17) Distefano, G.; Dal Colle, M.; Jones, D.; Zambianchi, M.; Favaretto, L.; Modelli, A. *J. Phys. Chem.* **1993**, *97*, 3504.
(18) Distefano, G.; de Palo, M.; Dal Colle, M.; Modelli, A.; Jones, D.; Favaretto, L. *THEOCHEM* **1997**, *418*, 99.
(19) Dal Colle, M.; Cova, C.; Distefano, G.; Jones, D.; Modelli, A.; Comisso, N. *J. Phys. Chem.* **1999**, *103*, 2828.
(20) Lane, N. F. *Rev. Mod. Phys.* **1980**, *52*, 29.
(21) Koopmans, T. *Physica* (*Amsterdam*) **1934**, *1*, 104.
(22) Heinrich, N.; Koch, W.; Frenking, G. *Chem. Phys. Lett.* **1986**, *124*, 20.
(23) Dal Colle, M.; Distefano, G.; Modelli, A.; Jones, D.; Guerra, M.; Olivato, P. R.; da Silva Ribeiro, D. *J. Phys. Chem. A* **1998**, *102*, 8037.
(24) Modelli, A.; Scagnolari, F.; Jones, D.; Distefano, G. *J. Phys. Chem. A* **1998**, *103*, 9675.
(25) Modelli, A.; Scagnolari, F.; Distefano, G. *Chem. Phys.* **1999**, *250*, 311.
(26) Cizek, J. *J. Chem. Phys.* **1966**, *45*, 4256.
(27) Sanche, L.; Schulz, G. J. *Phys. Rev. A*: *At., Mol., Opt. Phys.* **1972**, *5*, 1672.
(28) Modelli, A.; Jones, D.; Distefano, G. *Chem. Phys. Lett.* **1982**, *86*, 434.
(29) Johnston, A. R.; Burrow, P. D. *J. Electron Spectrosc. Relat. Phenom.* **1982**, *25*, 119.
(30) Scherer, O. J.; Wies, R. *Z. Naturforsch. B*: *Chem. Sci*. **1970**, *25*, 1486.
(31) Von Lidy, W.; Sundermeyer, W.; Verbeek, W. *Z. Anorg. Allg. Chem.* **1974**, *406*, 228.
(32) Baerends, E. J.; Ellis, D. E.; Ros, P. *Chem. Phys.* **1973**, *2*, 41.
(33) Vosko, S. H.; Wilk, L.; Nusair, M. *Can. J. Phys.* **1980**, *58*, 1200.
(34) Becke, A. D. *Phys. Rev. A*: *At., Mol., Opt. Phys*. **1988**, *38*, 3098.
(35) Perdew, J. P. *Phys. Rev. B*: *Condens. Matter* **1986**, *33*, 8822.
(36) Gustev, G. L.; Bartlett, R. J. *J. Chem. Phys.* **1996**, *105*, 8785.
(37) Parvis, G. D., III; Bartlett, R. J. *J. Chem. Phys.* **1982**, *76*, 1910.
(38) Frisch, M. J.; Trucks, G. W.; Schlegel, H. B.; Scuseria, G. E.; Robb, M. A.; Cheeseman, J. R.; Zakrzewski, V. G.; Montgomery, J. A., Jr.; Stratmann, R. E.; Burant, J. C.; Dapprich, S.; Millam, J. M.; Daniels, A. D.; Kudin, K. N.; Strain, M. O.; Farkas, O.; Tomasi, J.; Barone, V.; Cossi, M.; Cammi, R.; Mennucci, B.; Pomelli, C.; Adamo, C.; Clifford, S.; Ochterski, J.; Petersson, G. A.; Ayala, P. Y.; Cui, Q.; Morokuma, K.; Malick, D. K.; Rabuck, A. D.; Raghavachari, K.; Foresman, J. B.; Cioslowski, J.; Ortiz, J. V.; Stefanov, B. B.; Liu, G.; Liashenko, A.; Piskorz, P.; Komaromi, I.; Gomperts, R.; Martin, R. L.; Fox, D. J.; Keith, T.; Al-Laham, M. A.; Peng, C. Y.; Nanayakkara, A.; Gonzalez, C.; Challacombe, M.; Gill, P. M. W.; Johnson, B.; Chen, W.; Wong, M. W.; Andres, J. L.; Head-Gordon, M.; Replogle, E. S.; Pople, J. A. *Gaussian 98*, Revision A.6; Gaussian, Inc.: Pittsburgh, PA, 1998.
(39) Potts, A. W.; Price, W. C. *Proc. R. Soc. London, Ser. A* **1972**, *326*, 181.
(40) Cradock, S.; Whiteford, R. A. *J. Chem. Soc., Faraday Trans. 2* **1972**, *68*, 281.
(41) Szepes, L.; Koranyi, T.; Naray-Szabo, G.; Modelli, A.; Distefano, G. *J. Organomet. Chem.* **1981**, *217*, 35.
(42) Rabalais, J. W.; Colton, R. J. *J. Electron Spectrosc. Relat. Phenom.* **1972**, *1*, 83.
(43) Distefano, G.; Pignataro, S.; Ricci, A.; Colonna, F. P.; Pietropaolo, D. *Ann. Chim.* **1974**, *64*, 153.
(44) Horn, M.; Murrell, J. N. *J. Organomet. Chem.* **1974**, *70*, 51.
(45) Kobayashi, T.; Nagakura, S. *Bull. Chem. Soc. Jpn.* **1974**, *47*, 2563.
(46) Jordan, K. D.; Burrow, P. D. *Chem. Rev.* **1987**, *87*, 557.
(47) Modelli, A. *Trends Chem. Phys.* **1997**, *6*, 57.
(48) Guerra, M.; Distefano, G.; Jones, D.; Colonna, F. P.; Modelli, A. *Chem. Phys.* **1984**, *91*, 383.
(49) Modelli, A.; Distefano, G.; Jones, D. *Chem. Phys.* **1982**, *73*, 395.
(50) Modelli, A.; Venuti, M. *Int. J. Mass Spectrom.*, in press.
(51) Burrow, P. D.; Modelli, A.; Chiu, N. S.; Jordan, K. D. *Chem. Phys. Lett.* **1981**, *82*, 270.
(52) Beez, M.; Bock, H.; Heilbronner, E. *Helv. Chim. Acta* **1973**, *56*, 1028.
(53) Jones, T. B.; Maier, J. P. *Int. J. Mass Spectrom. Ion Phys.* **1979**, *31*, 287.
(54) Duke, C. B. In *Extended Linear Chain Compounds*; Miller, J. S., Ed.; Plenum Press: New York, 1982; Vol. 2, p 59.